Energy and Buildings 68 (2014) 242–253

Contents lists available at ScienceDirect

Energy and Buildings

journal homepage: www.elsevier.com/locate/enbuild

Modeling and control of color tunable lighting systems

Sina Afshari [a], Sandipan Mishra [b,*], Agung Julius [a], Fernando Lizarralde [c], John D. Wason [d], John T. Wen [a]

[a] Department of Electrical, Computer, and Systems Engineering, Rensselaer Polytechnic Institute, 110, 8th Street, Troy, NY 12180, USA
[b] Department of Mechanical, Aerospace, and Nuclear Engineering, Rensselaer Polytechnic Institute, 110, 8th Street, Troy, NY 12180, USA
[c] Department of Electrical Engineering, COPPE/UFRJ, P.O. Box 68504, CP 21945/970, Rio de Janeiro, Brazil
[d] Wason Technology, LLC, 740, Hoosick Road, Box 4117, Troy, NY 12180, USA

ARTICLE INFO

Article history:
Received 8 April 2013
Received in revised form 15 July 2013
Accepted 20 August 2013

Keywords:
Smart lighting
Feedback control
Energy efficiency
Intelligent buildings

ABSTRACT

Electric lighting has not substantially changed in over 100 years. From incandescent bulbs to fluorescent tubes, the efficiency remains low and control mostly involves on/off or dimming. The new wave of solid state lighting offers the possibility of sensor-based intensity regulation, color control, and energy efficiency, under varying needs and environmental conditions. This paper formulates the lighting control problem as an optimization problem balancing color fidelity, human perception and comfort, light field uniformity, and energy efficiency. The optimization problem is solved based on the light propagation model, which is adaptively updated with color sensor feedback to account for changing ambient lighting conditions, such as daylighting. We demonstrate the proposed approach in a smart space testbed under a variety of use conditions. The testbed is instrumented with 12 color tunable lights and 12 light sensors, as well as simulated daylight. The results show substantial improvement in terms of energy usage and delivering good light field quality in the presence of varying lighting conditions. Experimental results corroborate the efficacy of the proposed algorithms.

1. Introduction

Lighting is a major source of energy consumption in the U.S., using an estimated amount of more than 850 billion KWh annually in commercial sector, 16% of total electricity consumption of the country in this sector [1]. For the residential sector, this number is more than 550 billion KWh, 9% of the total electricity consumption of the country in this sector [1]. With the increasing importance of energy to economy and national security, solid state lighting (SSL) (i.e., light emitting diodes (LEDs) technology) is heralded as an important part of the solution as it offers energy efficiency and longevity. Indeed, the projected penetration of SSL into the lighting market would reduce energy usage by a whopping 49% [2]. SSL also possesses other attractive attributes including spectral tunability and fast response, which enables its use as a programmable device. These unique advantages of SSL open up a new dimension of lighting, called *smart lighting*, where lighting together with sensors creates an intelligent networked control system to achieve new levels of functionality, efficiency, and performance.

With the surging interest in SSL, there has been a rapidly growing body of related literature. Most of these efforts concentrate on novel material design, device packaging, and manufacturing. More recently, system-level research has been increasing due to the emphasis on overall systems-wide energy saving. Smart lighting control is typically posed as an optimization problem adjusting the individual light intensity to minimize energy consumption subject to task requirements, varying ambient lighting conditions (e.g., daylighting), and occupant locations. Most of this work regulates the intensity of white light to satisfy user needs while minimizing energy usage. The lighting specification is established based on the occupant locations and natural light distribution, which are measured by sensor networks consisting of light sensors and occupancy sensors or from measured usage data [3–8].

The system description used for lighting control is typically the light transport model [9], which relates light intensity of LEDs (of specified spectra) to the color (RGB) output at locations of interest. This model is static (i.e., no dynamics) and is used to determine light input to minimize some optimization objective, which would depend on occupancy, energy consumption, and account for the ambient light condition. Various optimization algorithms have been used for solving the optimal lighting problem, including linear programming [3,10], genetic algorithms [11,12], global search algorithms [13], and artificial neural networks [8]. Color tunable lights consisting of separately controlled multi-color LEDs have also been used to improve the photometric characteristics

* Corresponding author. Tel.: +1 510 7106507.
E-mail addresses: afshas@rpi.edu (S. Afshari), mishrs2@rpi.edu, sandipanmishra@gmail.com (S. Mishra), agung@ecse.rpi.edu (A. Julius), fernando@coep.ufrj.br (F. Lizarralde), wason@wasontech.com (J.D. Wason), wenj@rpi.edu (J.T. Wen).

0378-7788/$ – see front matter © 2013 Elsevier B.V. All rights reserved.
http://dx.doi.org/10.1016/j.enbuild.2013.08.036

[14,4,13,15–17] and achieve desirable color temperature [18,19]. However, several key challenges remain in realizing the promise of smart lighting systems, including reliable and adaptive light field estimation, assessment and interpretation of user requirements, and self-commissioning light fixtures.

As shown in the graphical abstract, the goal of this paper is to present a system-theoretic approach to smart lighting control of color-tunable lights under varying ambient lighting and room usage conditions, while balancing occupant comfort and energy consumption. We draw on color science to establish the basis for modeling, identification, and optimization of smart lighting systems. To address the issue of changing room conditions, occupancy, and ambient light levels, we propose an adaptive control approach. The efficacy of our approach is demonstrated on an experimental testbed consisting of multiple color tunable light fixtures, simulated daylighting, and color sensors.

Section 2 presents the mathematical definitions and concepts used in the formulation of lighting systems modeling and control problem. Section 3 poses the model identification, lighting control and adaptation problems as optimization problems. This section also suggests analytical solutions to these problems and discusses the convergence properties of the solutions. In Section 4, the experimental results obtained from implementing these control algorithms on an actual testbed are presented. Finally, Section 5 discusses the conclusions and future work while the appendix proves one of the statements made in Section 3.

2. Problem formulation

The light field at a point in space is characterized by the plenoptic function, $\phi(r, \theta, \lambda)$, which is the radiance along the ray given by the location of the point, $r \in \mathbb{R}^3$, and solid angle of the incoming light direction, $\theta \in S^2$, for the wavelength, $\lambda \in \Lambda$ where Λ is the visible light range [390, 750] nm [20].

Consider a space with n light fixtures each containing multiple adjustable intensity channels (p channels) represented as a vector $u_i \in \mathbb{R}^p$, $i = 1, \ldots, n$. Hence, there are pn control variables. Assume each control variable $u_i(j)$ is normalized to [0, 1].

Each light fixture generates a light-field distribution throughout the space. Let the unit (plenoptic) light field generated by fixture i be $S_i(r, \theta, \lambda) \in \mathbb{R}^p$ with the spectral dependence for each channel given by the spectral characteristics of the corresponding LED. Denote the ambient (uncontrolled) light field as $\psi(r, \theta, \lambda)$. Then the total light field is the linear combination of the two, based on the intensity levels of each fixture:

$$\phi(r, \theta, \lambda) = \sum_{i=1}^{n} S_i(r, \theta, \lambda)^T u_i + \psi(r, \theta, \lambda). \tag{1}$$

Assume there are m locations of interest for the light output. Because human color perception is based on three color-sensitive (red-green-blue, or RGB) photoreceptors (cones), we will consider $y_j \in \mathbb{R}^3$, consisting of the RGB measurements, $j = 1, \ldots, m$. The composite output vector is therefore a vector with $3m$ elements. Let light field weighting function for each sensor be $C_j(r, \theta, \lambda) \in \mathbb{R}^3$. The output at each location is therefore given by

$$y_j = \langle C_j, \phi \rangle + v_j \tag{2}$$

where $\langle \cdot, \cdot \rangle$ denotes integration over the spatial, angular, and spectral ranges of the light sensor, and v_j is the sensor noise. For a point light sensor at r_j, the r dependence in C_j is just $\delta(r - r_j)$. The θ dependence corresponds to the angular sensitivity, typically governed by the sensor optics. The spectral dependence is based on the spectral characteristics of the RGB sensor channels.

Substituting the light field (1) into the sensor equation (2), we get

$$y = Pu + w + v \tag{3}$$

where $y \in \mathbb{R}^{3m}$ is the output light measurement vector, $u \in \mathbb{R}^{pn}$ the input light intensity control vector, $P \in \mathbb{R}^{3m \times pn}$ is the *light transport matrix* with the (j, i)th $3 \times p$ submatrix given by $\langle C_j, S_i^T \rangle$, $w \in \mathbb{R}^{3m}$ is the ambient light with $w_j = \langle C_j, \psi \rangle$, and $v \in \mathbb{R}^{3m}$ the measurement noise vector.

We pose the lighting control problem as the adjustment of u to balance between the desired y, determined by occupants' needs and comfort, and the power consumption by the lights. First, input/output data is used to identify the light transport matrix. A cost function consisting of a weighted sum of power consumption and lighting quality is then constructed. A gradient projection method that aims to minimize this cost is then employed to update u based on the feedback of the output measurement y. In the presence of unknown external light disturbances and changing light transport properties in the room, we apply adaptive algorithms to improve the robustness of the control scheme. The desired lighting y_d depends on the location of occupants and spatial uniformity requirement. A key issue is the determination of an appropriate quality metric for color tunable lighting, for which human visual perception and comfort must be considered.

For spatial uniformity, we draw from existing literature in formation control [21] by considering the lights as an undirected graph. Each light is connected to its neighboring lights by links (neighbors may be defined as all lights within certain distance). We arbitrarily assign an orientation to the graph by designating one of the two nodes of a link to be the positive end. Denote by $\mathcal{L}_i^+$ ($\mathcal{L}_i^-$) the set of links for which node i is the positive (negative) end. Let the total number of links be ℓ. Then the incidence matrix $D \in \mathbb{R}^{n \times \ell}$ of the graph is defined by

$$d_{ik} = \begin{cases} +1 & \text{if } k \in \mathcal{L}_i^+ \\ -1 & \text{if } k \in \mathcal{L}_i^- \\ 0 & \text{otherwise.} \end{cases} \tag{4}$$

We shall use this graph as the basis for addressing light uniformity.

3. Optimal lighting control

3.1. Model identification

Measured input–output data may be used to identify the (static) light transport matrix, P. The typical approach [22] is a linear least squares fit to input–output data. Let $U = [u_1\, u_2 \ldots u_N]$ be a sequence of light inputs and $Y = [y_1\, y_2 \ldots y_N]$ be the corresponding measured outputs. In the absence of disturbance light, the least squares estimate of P is simply $\hat{P} = YU^+$ where U^+ is the Moore–Penrose pseudo-inverse of U. If the noise characteristics vary between sensors, a weighting matrix may be included in the least squares problem. Usual caution for least squares identification should always be exercised to ensure U is of full row rank and well conditioned (typical approach is to use randomly generated u).

However, the output consists of RGB measurements and it is well known that the Euclidean norm in the RGB space does not reflect the color sensitivity of human perception [23]. To mimic human perceptual uniformity, a common choice is the *Lab* color representation as defined in [24] (see Appendix A) which is a nonlinear transformation of the RGB space. We therefore pose

the model identification problem as an optimization using the Euclidean norm in *Lab*-space

$$\min_P \sum_{i=1}^{m} \|f(y_i) - f(P_i u)\|^2 = \min_P \left\| f(y) - f(Pu) \right\|^2 \tag{5}$$

where $f : \mathbb{R}^3 \to \mathbb{R}^3$ is the mapping from RGB to *Lab* (with components denoted by f_L, f_a, f_b, respectively), and P_i is the 3-row submatrix of P that corresponds to y_i. We will use the notation $f(y)$, $y \in \mathbb{R}^{3m}$ to denote the vector consisting of $[f(y_1)^T, \ldots, f(y_m)^T]^T$ with $y_i \in \mathbb{R}^3$, $i = 1, \ldots, m$. This is a nonlinear optimization problem and a closed form solution is not readily available as in the linear least squares problem. Since f is an isomorphism between RGB and *Lab* color spaces (i.e., f' is nonsingular (see Appendix A)), the optimization remains convex. Hence, any gradient iteration will guarantee convergence.

3.2. Lighting optimization problem

Given the light transport model (3), we pose the lighting control problem as an optimization of the input u to minimize a linear combination of three terms: a light quality metric, μ_Q, a power consumption metric, μ_E, and a spatial uniformity metric, μ_S.

Suppose a desired color and luminance is specified for each sensor, represented together as a vector y_{des}, we can simply use the weighted Euclidean norm in the *Lab* space as the output light metric

$$\mu_Q = \sum_{i=1}^{m} (f(y_i) - f(y_{i_{des}}))^T \Gamma_Q^{-1} (f(y_i) - f(y_{i_{des}})) \tag{6}$$

where Γ_Q is a positive definite (typically diagonal) weighting matrix.

The power consumption metric characterizes the power consumed by the lighting fixtures as a function of the light intensity vector, u. Assuming linear efficiency of the power converters used in the LED driver circuit and taking into account the different LED efficiencies, we choose μ_E as

$$\mu_E = \Gamma_E^{-1} u = \sum_{i=1}^{pn} \gamma_i^{-1} u_i \tag{7}$$

where γ_i is the efficiency of lighting control channel i.

The human eye is sensitive to spatial non-uniformity in both luminance and chromaticity. To avoid large color variations between the lights due to an ill-conditioned P, we will penalize the color difference between neighboring lights in the optimization problem. Define the lighting difference variable z_k as

$$z_k = \sum_{i=1}^{n} d_{ik}(u_i) = \begin{cases} u_i - u_j & \text{if } k \in \mathcal{L}_i^+ \\ u_j - u_i & \text{if } k \in \mathcal{L}_i^- \end{cases} \tag{8}$$

where u_j is the light that connects to u_i via link k.

Following the approach in [21], partition the incidence matrix, D from (4), in terms of column vectors:

$$D = [D_1 \quad \ldots \quad D_\ell].$$

Then

$$z_k = (D_k^T \otimes I)u.$$

Stacking all the z_k's together as a column vector, we have

$$z = (D^T \otimes I)u. \tag{9}$$

We choose the spatial uniformity metric as the Euclidean norm of z:

$$\mu_S = \|z\|. \tag{10}$$

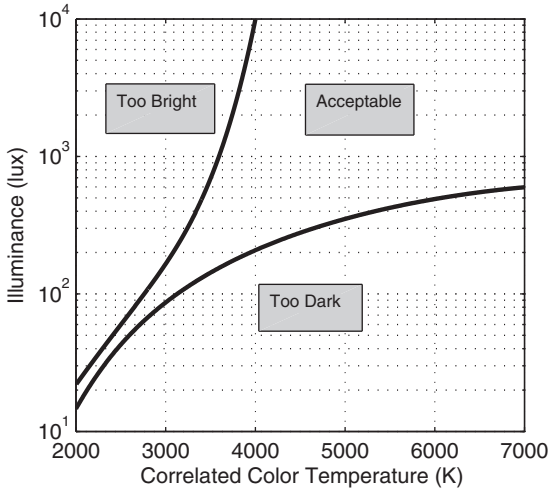

Fig. 1. The Kruithof curve used in this work as a criterion to capture the human comfort factor.

We pose the overall optimization problem as choosing the light input to minimize the weighted sum of the three metrics:

$$\begin{aligned} &\min_{u \in \mathcal{U}} J(u) \\ &J(u) = \alpha_Q \mu_Q(Pu, y_{des}) + \alpha_E \mu_E(u) + \alpha_S \mu_S(u). \end{aligned} \tag{11}$$

Note we ignore the ambient light w and sensor noise v for the optimization problem. We will address their effect on specific lighting control strategies in the next section.

In addition to spatial color uniformity, there are numerous other factors for the human comfort level affected by the lighting system such as brightness level, color, glare, and flicker [25]. For white light, i.e., restricting the chromaticity to be on the Planckian locus, the range of "comfortable" lighting parameterized by luminance and color temperature is captured by an empirical curve called Kruithof curve [26]. For a given luminance, L, the Kruithof curve gives the range of color temperature, denoted by $T_k(L)$, that has been empirically determined to be comfortable to average human occupants, as shown in Fig. 1. In this case, we consider the problem where the user only specifies the luminance (e.g., via dimmer control) and the desired color temperature is only restricted to be in the range given by the Kruithof curve. Our approach is to first determine the desired color temperature that minimizes power consumption given the desired luminance at each output $f_L(y_{i_{des}})$:

$$\begin{aligned} &\min_u \mu_E(u) \quad \text{such that} \\ &CCT(f_a(y_i), f_b(y_i)) \in T_k(f_L(y_{i_{des}})),\ i = 1, \ldots, n \\ &y = Pu + w. \end{aligned} \tag{12}$$

where CCT denotes the color temperature function for a given color parameterized by ab. The resulting solution, $(f_a(y^*), f_b(y^*))$ is then used together with $f_L(y_{des})$ as the color setpoint for (11).

3.3. Lighting control

3.3.1. Model-based optimization

All three metrics in (11) are (locally) convex in u. The stationarity condition for μ_Q, $\nabla_u \mu_Q = 0$, is only satisfied at $Pu = y_{des}$, and the Hessian $\nabla_u^2 \mu_Q$ is positive definite at that point (based on f' being nonsingular, shown in Appendix A). A similar argument shows the uniformity metric μ_S is also convex. The power consumption metric μ_E is linear in u, and is therefore convex. The constraint set for u is also convex. Therefore, any gradient update law may be used to ensure convergence to the optimum (which may not be unique). For

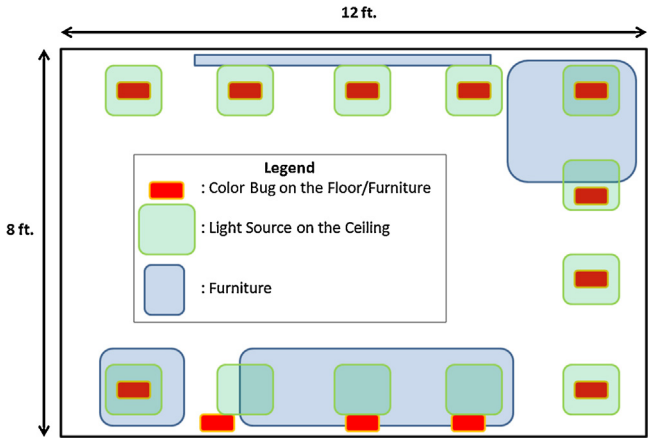

Fig. 2. The layout of furniture, light sources and sensors in the lighting control testbed.

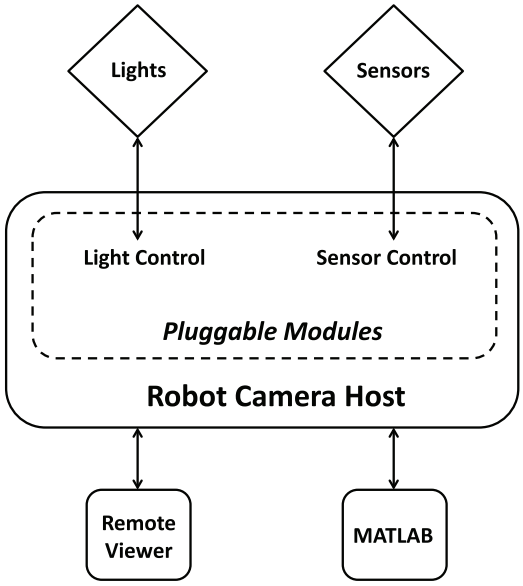

Fig. 3. Schematic of distributed control and communication architecture used in the lighting control testbed based on Robot Raconteur.

simplicity, we will use gradient update with projection for updating the lighting control:

$$u_{k+1} = P_{\mathcal{U}}[u_k - K(\alpha_L P^T f'^T(y_k)\Gamma_Q^{-1}(f(y_k) - f(y_{des})) + \alpha_E \Gamma_E^{-1} + \alpha_S(f_a'^T(u_k)DD^T f_a(u_k) + f_b'^T(u_k)DD^T f_b(u_k)))] \quad (13)$$

where $P_{\mathcal{U}}$ is the projection to ensure the lighting control is within the allowed range. Note that w and v do not need to be known explicitly. As long as they are constants, the iterative algorithm will converge to an optimum value. If the sensor noise characteristics is non-uniform, i.e., the noise covariance is not a scaled identity matrix, it may be incorporated into the gradient update [27].

3.3.2. Model adaptation

In the gradient algorithm above, we have assumed that P and w are constants. In case that P and w are uncertain or time varying, such as under changing occupancy and ambient light condition, we may estimate P and w through the standard least squares optimization problem:

$$\begin{aligned} &\min_{P,w}(y - (Pu + w))^T \Sigma_V (y - (Pu + w)) \\ &= \min_{\Phi}(y - \Phi a)^T \Sigma_V (y - \Phi a), \\ &\text{where } \Phi = [u^T \otimes I_{m\times m} \quad I_{m\times m}], \quad a = \begin{bmatrix} \text{vec}(P) \\ w \end{bmatrix} \end{aligned} \quad (14)$$

where Σ_V is the sensor noise covariance.

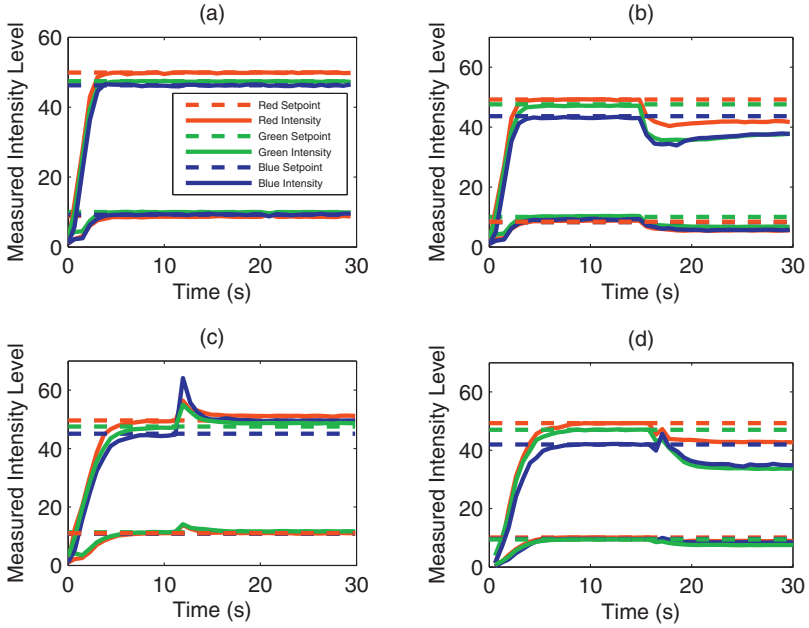

Fig. 4. Convergence of different components of the measured lighting condition (solid lines) to their setpoints (dashed lines) for sensor #5. (a) No external light (disturbance) and no weighting on energy, (b) no disturbance with weighting on energy, (c) with disturbance and no weighting on energy, (d) with disturbance and weighting on energy.

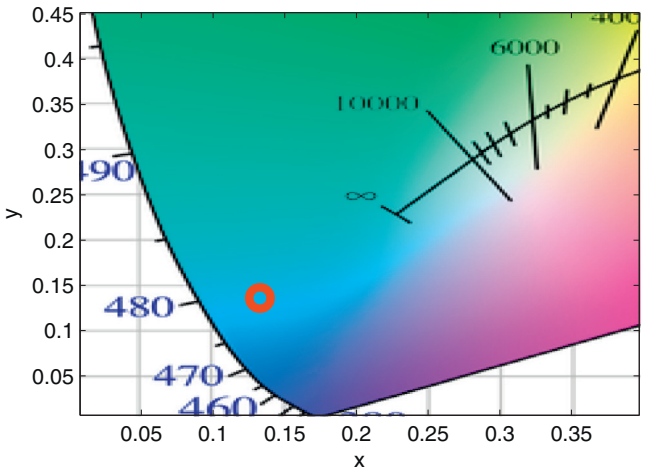

Fig. 5. The chromaticity of the external (disturbance) light.

There are numerous recursive algorithms to solve this problem [27]. We choose the recursive least squares update in our implementation:

$$\begin{aligned} \hat{a}_{k+1} &= \hat{a}_k + K_k(y_k - \Phi_k \hat{a}_k) \\ K_k &= L_{k-1}\Phi_k^T(\Phi_k L_{k-1}\Phi_k^T + \beta\Sigma_V)^{-1} \\ L_k &= \beta^{-1}(I - K_k\Phi_k)L_{k-1}. \end{aligned} \tag{15}$$

where $\beta \in (0, 1)$ is the forgetting factor to allow tracking of time varying P and w.

4. Experimental results

4.1. Testbed description

We have constructed a lighting control testbed to demonstrate and validate lighting control schemes [28]. This testbed is a furnished $8' \times 12' \times 8'$ room with windows and an overhead backlight unit to simulate a skylight. The room has twelve 7″ round downlight fixtures by Acuity [29]. Each light has individually controllable RGB channels (with input range [0,1]). There are also twelve Seachanger wireless color sensors by Ocean Optics providing RGB intensity measurements [30]. A schematic floor plan layout of the testbed with furniture, light sources and sensors is shown in Fig. 2. A tungsten filament projector lamp simulates sunlight coming in through the window. The intensity of the ceiling backlighting is adjustable (approximately 65–650 lux). The lights and sensors are connected via a local area network to a server. This sensor/actuator network is supported by an open source distributed communication and control software system, *Robot Raconteur*, developed at Rensselaer Polytechnic Institute, originally in support of robotics research [31]. It allows a seamless integration of these devices and provides ready interface to data analysis software such as MATLAB (in which all control and analysis algorithms are implemented). The overall control and communication architecture is shown in Fig. 3.

4.2. Optimization-based control

First consider just the color metric alone, $\alpha_E = \alpha_S = 0$,with the identified light transport matrix P. We use the method discussed in 3.1 to obtain P (The average residual error on a verification set of 300 samples is equal to 3.83%). For feedback control, we choose $CCT = 4000$ K as a typical comfortable lighting setpoint. As expected the measurements converge to the setpoint in about 3 sec as shown in Fig. 4(a). The desired chromaticity and generated chromaticity are almost indistinguishable as shown in Fig. 6(a) and (b). The

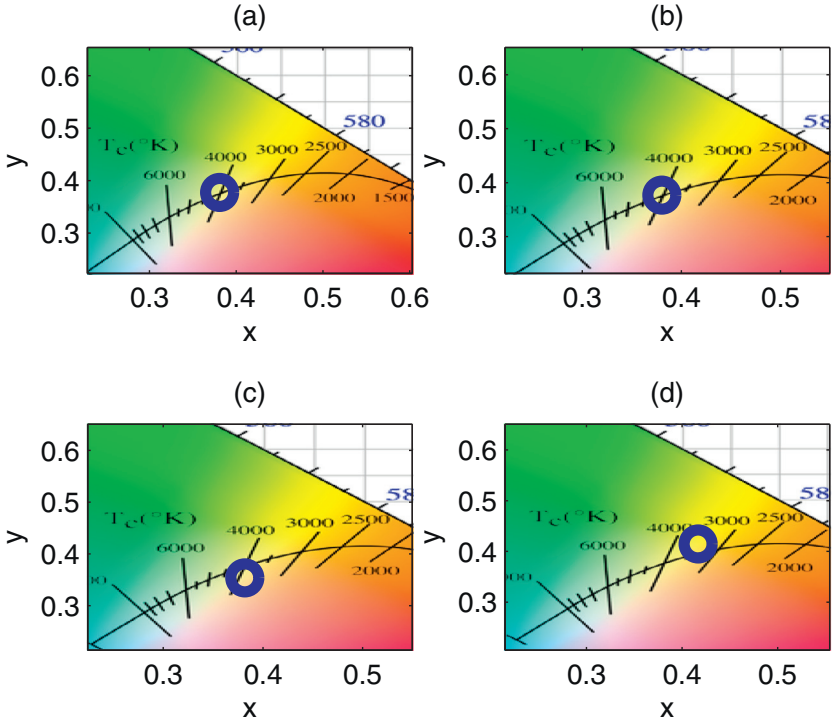

Fig. 6. (a) Desired chromaticity of the generated light, (b) actual chromaticity of the generated light for the cases with no disturbance and no weighting on energy, (c) no disturbance with weighting on energy, (d) with disturbance and no weighting on energy.

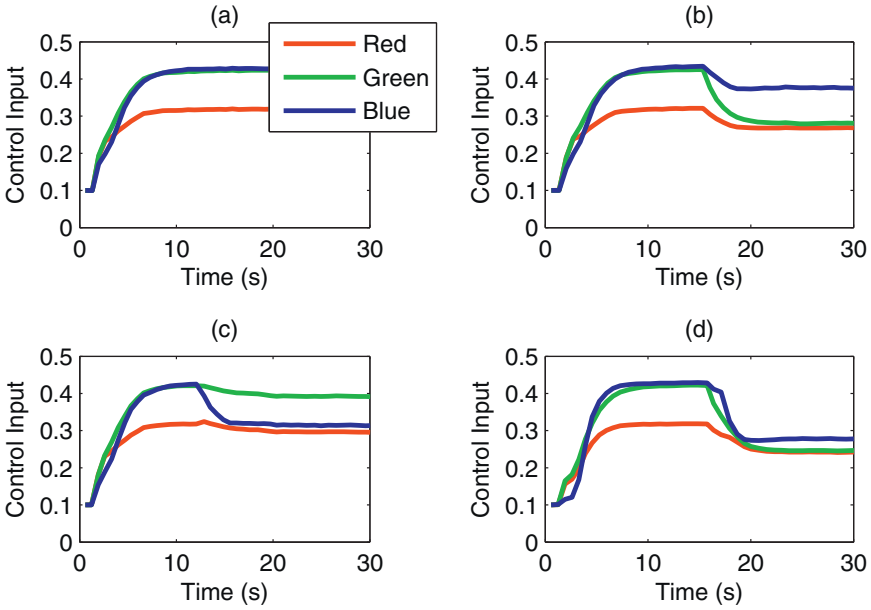

Fig. 7. Control input of the system for different experiments for source #5. (a) No disturbance no weighting on energy, (b) no disturbance with weighting on energy, (c) with disturbance no weighting on energy, (d) with disturbance and weighting on energy.

control input is shown in Fig. 7(a). The power consumption is shown in Fig. 8(a).

When the α_E is changed from 0 to 0.04 (at $t = 15$ s), the power consumption is quickly reduced by 20% as shown in Fig. 8(b). This is also reflected in the lower control effort as in Fig. 7(b). The measured color moves slightly away from the desired setpoint as shown in Fig. 4(b) and the overall brightness is decreased. For the generated light, u, the direction of the shift is determined by Γ_E, here moving away from the green part of the diagram due to the lower efficiency of the green LEDs. Further power reduction may be achieved by increasing α_E but at the expense of larger deviation from the color setpoint.

We next consider the effect of ambient lighting by turning on the backlight at the lowest intensity (65 lux). This unmodeled disturbance light is mostly in the blue range as shown in Fig. 5. After an initial transient, the controller quickly adjusts itself (reducing the blue content as shown in Fig. 7(c), with chromaticity shown in Fig. 6(d)) to maintain the color setpoint, shown in Fig. 4(c). The setpoint is not attained perfectly as in the disturbance-free case, as w is not completely within the range of P and therefore cannot be fully cancelled by the light input. Because the reduced demand on the generated blue light, the overall power consumption is reduced by 20% as shown in Fig. 8(c) – with very little sacrifice of color fidelity, in contrast to increasing α_E. The controller essentially *harvests* the

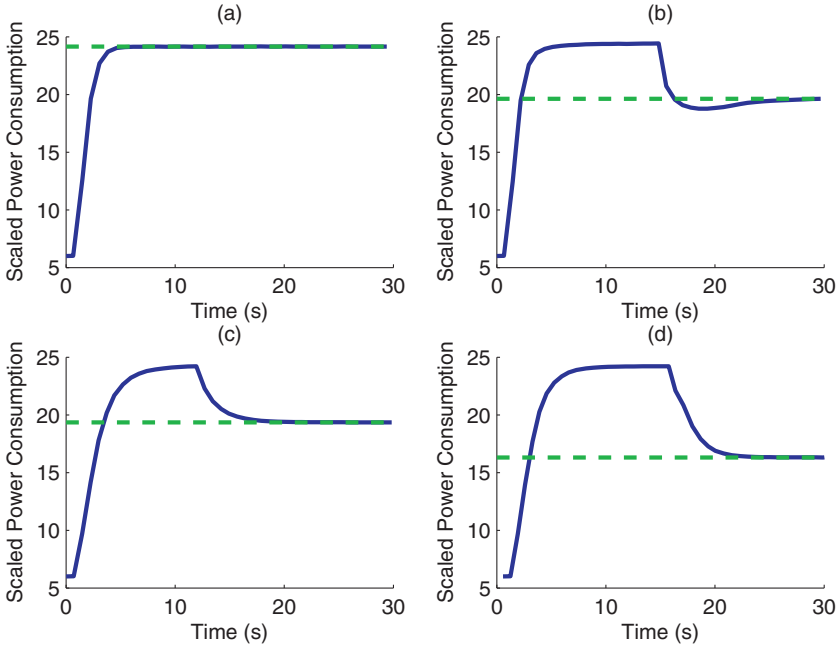

Fig. 8. Scaled power consumption (solid lines) for different experiments compared to their steady state values (dashed lines). (a) No disturbance and no weighting on energy, (b) no disturbance with weighting on energy, (c) with disturbance and no weighting on energy, (d) with disturbance and weighting on energy.

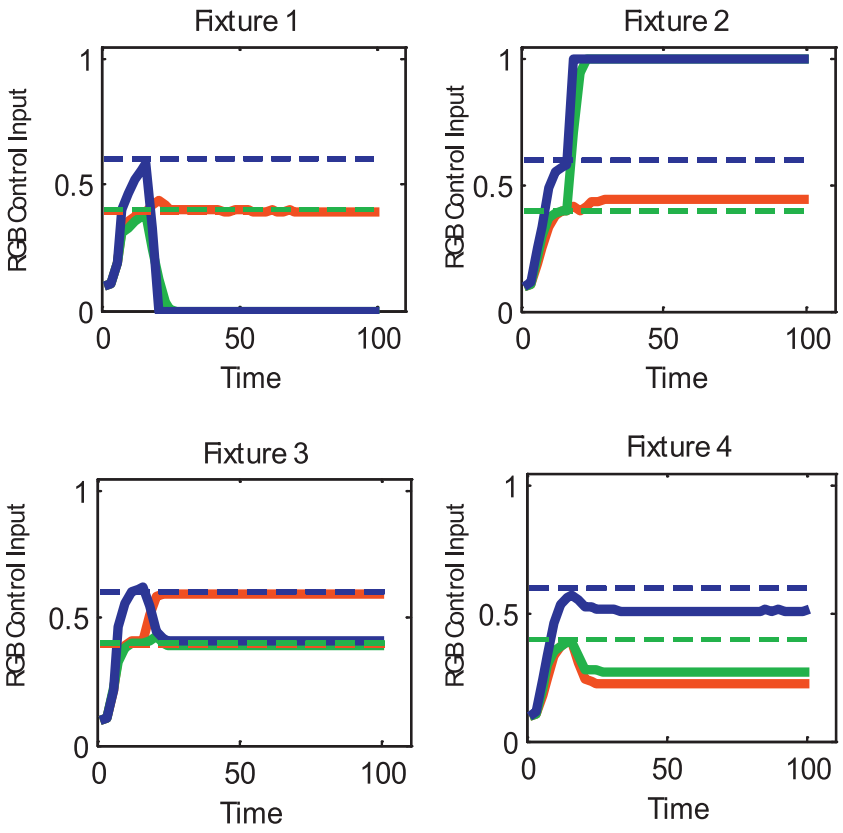

Fig. 9. Light intensity control input without uniformity cost. An amber filter is placed in front sensor #2 at $t = 10$ s.

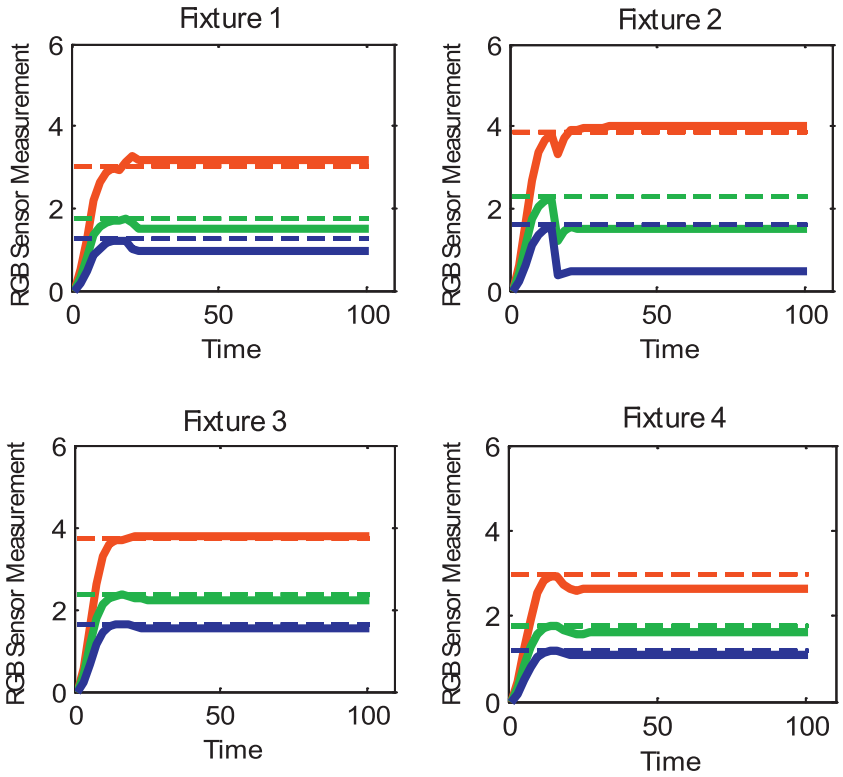

Fig. 10. Light sensor measurements (solid lines) under lighting control without uniformity cost compared to the setpoints (dashed lines). An amber filter is placed in front sensor #2 at $t = 10$ s. The setpoints are different for different sensors because in this experiment, they were placed in different heights.

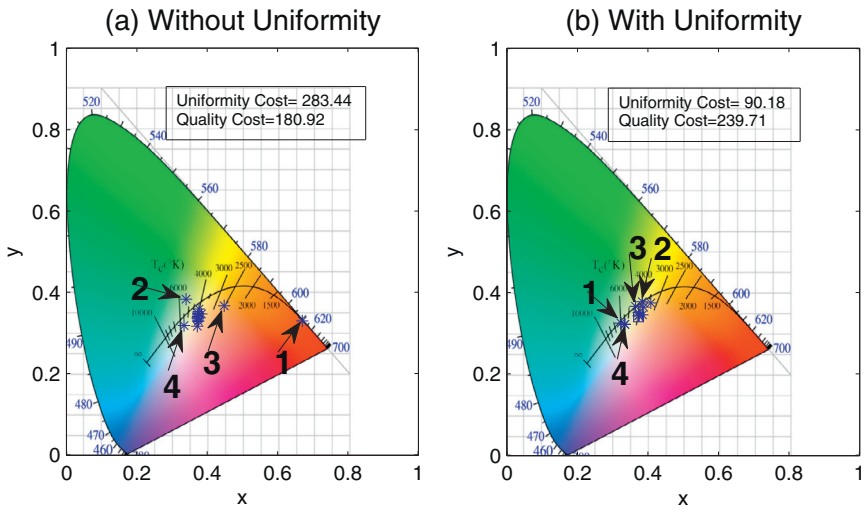

Fig. 11. The chromaticities of control input of different light fixtures (a) for no uniformity cost and (b) with uniformity cost.

ambient light to achieve the lighting objective by using less controlled lighting. When both ambient light and power consumption penalty are present, we see the most amount of power reduction, by 40%, as shown in Fig. 8(d). The color performance is similar to the power-penalized case.

4.3. *Effect of the uniformity metric*

The graph formed by the lights in our testbed is a simple chain. The difference variable z is therefore just the difference between the inputs to adjacent lights. To show the effect of spatial uniformity weight, α_S, we consider the case where the desired output corresponds to all lights with identical inputs of $[0.4, 0.4, 0.6]^T$. We then place an amber filter in front of sensors #2 at $t = 10$ s to introduce an error in P. We first consider the case without the uniformity weighting, i.e., $\alpha_S = 0$. Initially, all outputs converge to the desired values and the input for each light converges to the same value. When the disturbance is introduced at $t = 10$ s, the light intensities in LEDs #1 and 2 saturate, trying their best to compensate for the amber filter. As a result, there is large color variation for lights 1 to 4, as shown in Fig. 9. The corresponding output measurements are shown in Fig. 10, with sensor 2 showing large color error, but the other sensors are close to the setpoint. The effect of lighting control to compensate for the disturbance may also be seen in the chromaticity diagram in Fig. 11(a), particularly for lights in the region near the sensor with the amber filter (lights 1–4). Though the color measurements at the sensors are relatively close to their setpoints, the large color variation between adjacent lights can

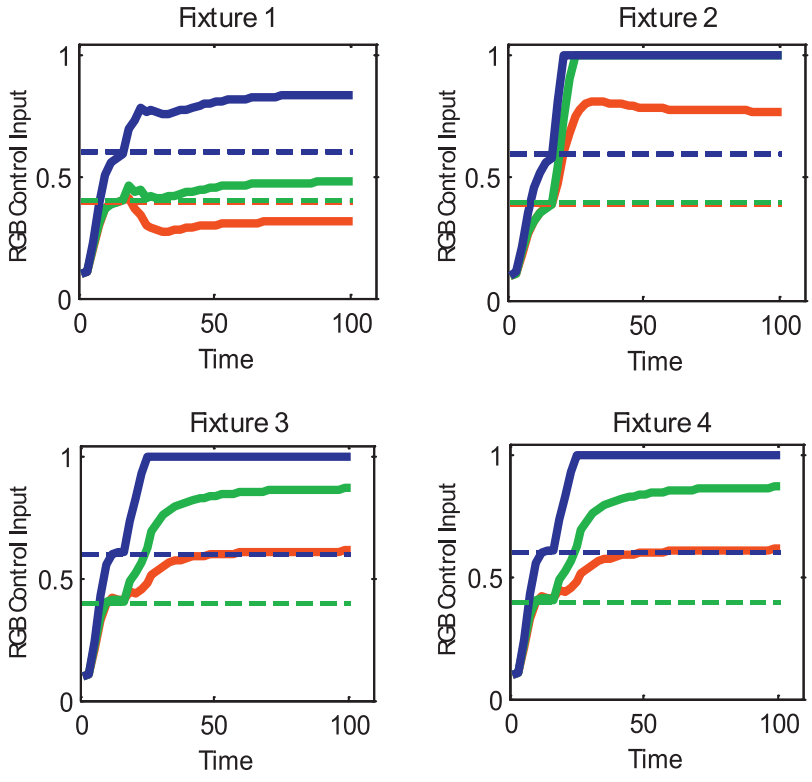

Fig. 12. Light intensity control input with uniformity cost. An amber filter is placed in front sensor #2 at $t = 10$ s.

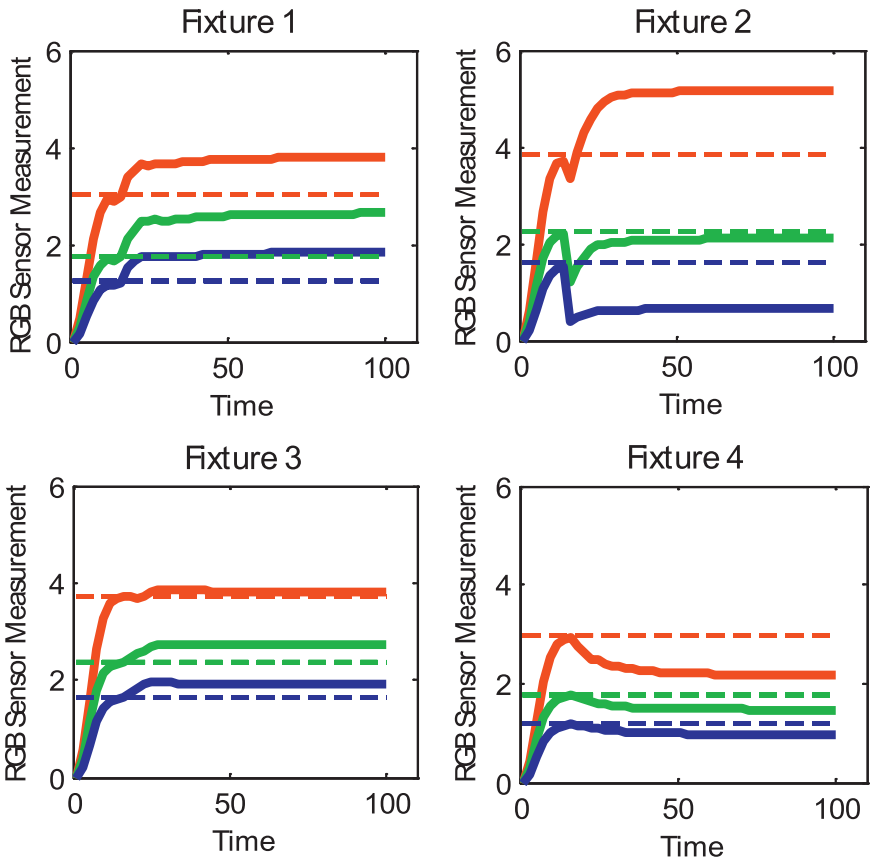

Fig. 13. Light sensor measurements (solid lines) under lighting control with uniformity cost compared to the setpoints (dashed lines). An amber filter is placed in front sensor #2 at $t = 10$ s.

be uncomfortable to the occupants. When the uniformity cost is introduced, neighboring lights now have closer colors, as shown in terms of the normalized RGB values in Fig. 12 and chromaticity in Fig. 11(b). The chromaticities of the generated light from different fixtures cluster more closely together in this case, resulting in more spatial uniformity of colors of the light fixtures, in exchange for poorer output light quality. This experiment shows 68% decrease in the uniformity cost, in exchange for 32% increase in the quality cost.

4.4. Kruithof-based control

For white light illumination, only the neighborhood of the Planckian locus, parameterized by color temperature, in chromaticity is considered. For a specified luminance, the Kruithof curve [26] provides the range of color temperatures comfortable to human occupants. We determine the specific color temperature setpoint in the range that minimizes power consumption. For our experiment, we set the target luminance to 400 lux; the corresponding

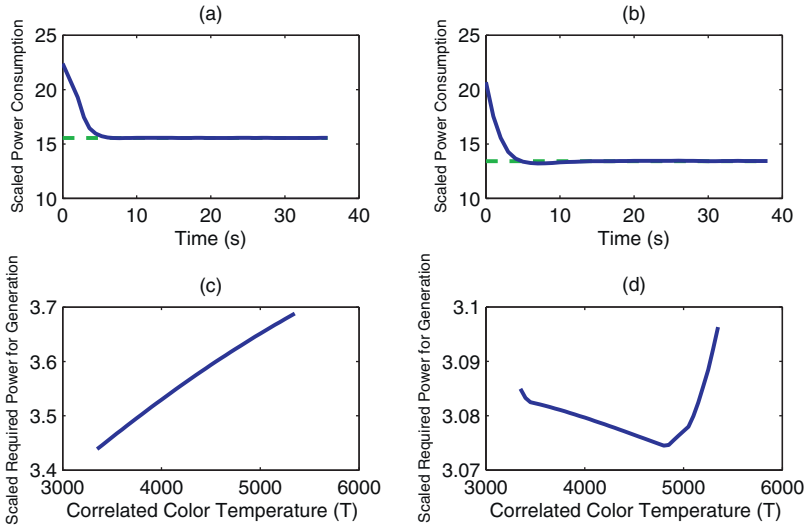

Fig. 14. Scaled power consumption (solid lines) compared to the steady state value (dashed lines) for the two experiments: (a) without disturbance and (b) with disturbance. The required power for generation of the light with different CCTs for the two experiments, (c) without disturbance and (d) with disturbance.

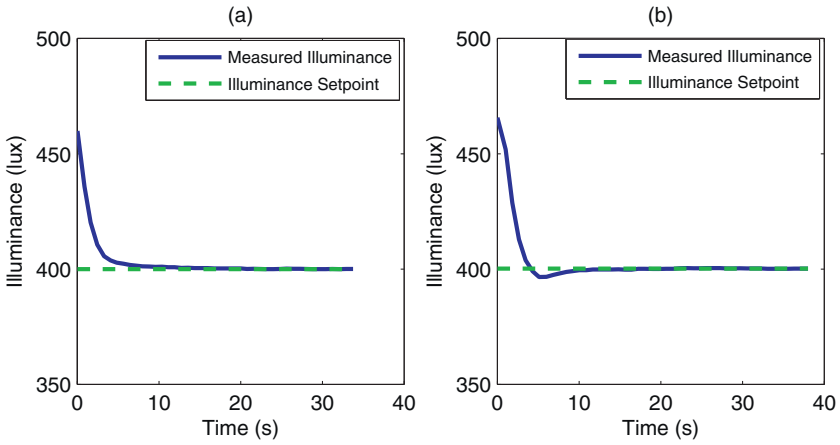

Fig. 15. Convergence of the illuminance level (solid lines) to its setpoint (dashed lines) in the two experiments: (a) without disturbance and (b) with disturbance.

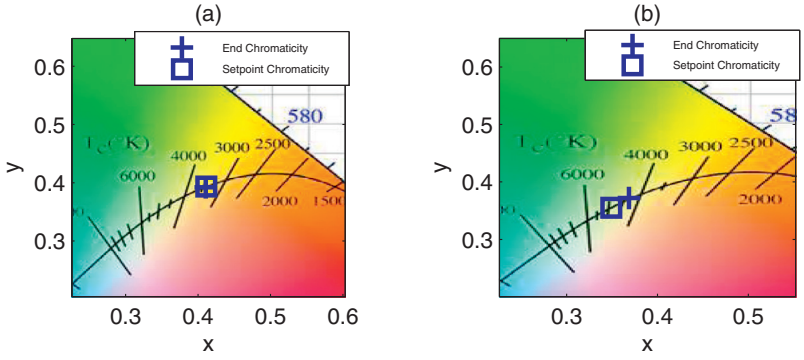

Fig. 16. Desired chromaticity of the generated light compared to that of the setpoint for the two experiments: (a) without disturbance and (b) with disturbance.

color temperature interval based on the Kruithof curve is [3500 K, 5500 K].

Fig. 13.

In the absence of ambient light disturbance, the most energy efficient CCT is 3500 K, as shown in Fig. 14(c). This provides the color setpoint to the optimization-based controller. The power consumption and convergence of the luminance are shown in Figs. 14(a) and 15(a), respectively. Since there is no ambient light disturbance, the chromaticity of the generated light exactly corresponds to the specified color temperature as shown in Fig. 16(a).

When a low level, 65 lux, of ceiling simulated skylight is present (same as in the optimization-based control experiments), the most energy efficient color temperature is now 4900 K as shown in Fig. 14(d). This is due to the dependence of the optimal color temperature on the spectral content of ambient disturbance light. In our experiment, the ambient light has a strong blue component.

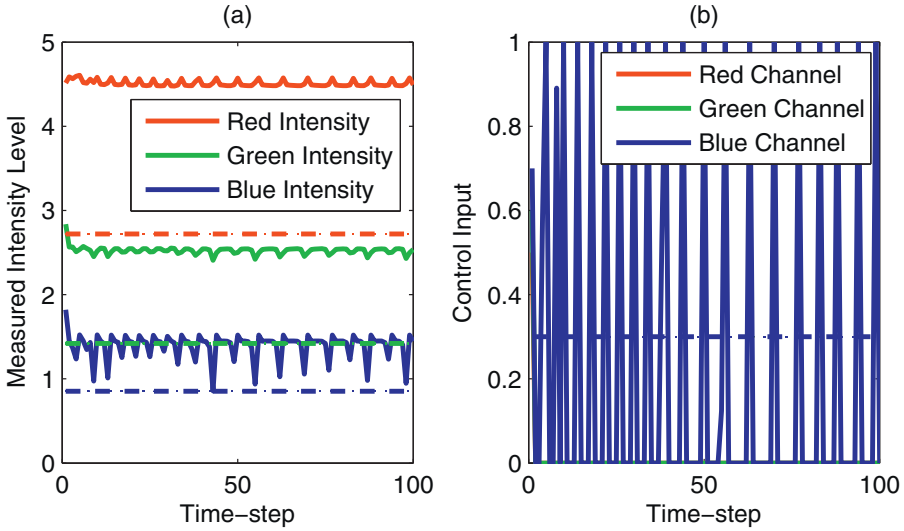

Fig. 17. (a) The sensor measurements (solid lines) compared to their setpoints (dashed lines) and (b) control input for sensor #2 for the case without model adaptation.

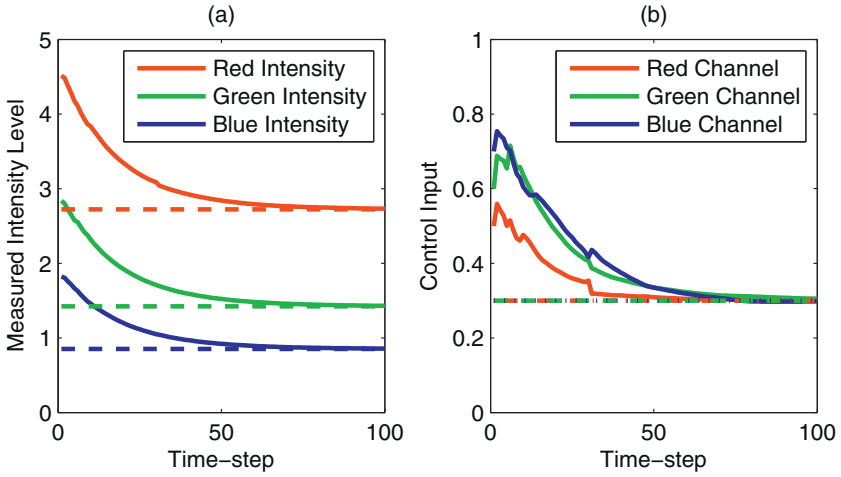

Fig. 18. (a) The sensor measurements (solid lines) compared to their setpoints (dashed lines) and (b) control input for sensor #2 for the case with model adaptation.

The optimal setpoint takes advantage of the availability of the blue content, resulting in a higher color temperature. The power consumption and convergence of the luminance are shown in Figs. 14(b) and 15(b), respectively, showing 20% power reduction in the disturbance case similar to the optimization-based case.

4.5. Feedback control with model adaptation

In many cases, the light transport model may not be well-identified or may change over time. In this section, we show that light transport model adaptation may be critical to maintain stability of the closed loop lighting control. As an example, instead of the identified light transport model, we use an erroneous model (specifically, P identified in (5) with sensor #2 covered) in the feedback control law (13), with and without model adaptation. In the nonadaptive case, the modeling error causes the closed loop system to become unstable, as shown in Fig. 17. In the adaptive case, the light propagation matrix P and the disturbance light input w are updated at each time instant, and the updated model is then used for feedback control. The closed loop stability is restored as shown in Fig. 18.

5. Conclusion and future work

This paper presents a systematic approach to the modeling, optimization, control, and adaptation in a color-tunable LED lighting control system. Through light sensor feedback, the control system is able to achieve significant energy savings without substantially sacrificing lighting quality. The key conclusions from this research are:

- By appropriate choice of cost function based on color metrics, the trade-off between quality of light and energy consumption for LED lighting systems may be achieved.
- Disturbance light (daylight) may be harvested to reduce power consumption while maintaining light quality.
- Human comfort factors can be included through empirical characterizations such as the Kruithof curve.
- Recursive update of the light transport matrix using input and output data improves lighting control performance.

Current research directions include distributed deployment and control to facilitate commissioning in existing or new infrastructure, and integration with other building control systems such as heating, cooling, and air quality control.

Acknowledgments

This work was supported primarily by the Engineering Research Centers Program (ERC) of the National Science Foundation under NSF Cooperative Agreement No. EEC-0812056, and in part by the NSF-CHE 1230687 SEP Collaborative grant, HP Lab IRP Award, and New York State Foundation for Science, Technology and Innovation (NYSTAR) under contracts C080145 and C090145. The authors gratefully acknowledge helpful discussion and assistance of Professors Arthur Sanderson and Robert Karlicek.

Appendix A. Nonsingularity of f

Definition: Let $[R\,G\,B]^T \in \mathbb{R}^3$ be the representation of a color in RGB space, and $[X, Y, Z]^T$ be obtained through an invertible linear transformation T on $[R\,G\,B]^T$

$$\begin{bmatrix} X \\ Y \\ Z \end{bmatrix} = \begin{bmatrix} 2.7688 & 1.7517 & 1.1301 \\ 1 & 4.5906 & 0.0601 \\ 0 & 0.0565 & 5.5942 \end{bmatrix} \begin{bmatrix} R \\ G \\ B \end{bmatrix}. \tag{A.1}$$

The Lab representation of the color, $Lab = [L, a, b]^T$, is then determined from the following nonlinear transformation

$$\begin{aligned} L &= 116 g\left(\frac{Y}{Y_n}\right) - 16 \\ a &= 500\left(g\left(\frac{X}{X_n}\right) - g\left(\frac{Y}{Y_n}\right)\right) \\ b &= 200\left(g\left(\frac{Y}{Y_n}\right) - g\left(\frac{Z}{Z_n}\right)\right). \end{aligned} \tag{A.2}$$

X_n, Y_n and Z_n are the XYZ tristimulus values of the reference white point and the function $g(t)$ is defined as below

$$g(t) = \begin{cases} t^{\frac{1}{3}} & \text{if } t > \left(\frac{6}{29}\right)^3 \\ \frac{1}{3}\left(\frac{29}{6}\right)^2 t + \frac{4}{29} & \text{Otherwise.} \end{cases} \tag{A.3}$$

$g(t)$ can easily be shown to be continuous, once differentiable and $g'(t) \neq 0 \quad \forall t$.

Proposition: Let $f : \mathbb{R}^3 \to \mathbb{R}^3$ be the mapping from RGB to Lab, then, $f' \in \mathbb{R}^{3\times 3}$ is always nonsingular.

Proof: We first show that f is always differentiable. f' can be written as

$$f' = T \times \begin{bmatrix} 0 & \frac{116}{Y_n} g'\left(\frac{Y}{Y_n}\right) & 0 \\ \frac{500}{X_n} g'\left(\frac{X}{X_n}\right) & -\frac{500}{Y_n} g'\left(\frac{Y}{Y_n}\right) & 0 \\ 0 & \frac{200}{Y_n} g'\left(\frac{Y}{Y_n}\right) & -\frac{200}{Z_n} g'\left(\frac{Z}{Z_n}\right) \end{bmatrix} \quad \text{(A.4)}$$

and since g is continuous and once differentiable, f' always exists. Also, the determinant of f' is

$$|f'| = \frac{7.1178 \times 10^7}{X_n Y_n Z_n} g'\left(\frac{X}{X_n}\right) g'\left(\frac{Y}{Y_n}\right) g'\left(\frac{Z}{Z_n}\right) \quad \text{(A.5)}$$

which is always nonzero. Therefore, f' is nonsingular. □

References

[1] EIA, Annual energy outlook 2013 early release. Technical Report DOE/EIA-0383ER(2013), 2012, December.
[2] DOE, Life-cycle assessment of energy and environmental impacts of led lighting products. Technical report, 2012, February.
[3] Y.J. Wen, J. Granderson, A.M. Agogino, Towards embedded wireless-networked intelligent daylighting systems for commercial buildings, in: International Conference on Sensor Networks, Ubiquitous, and Trustworthy Computing, vol. 1, 2006, pp. 326–331.
[4] M. Aldrich, N. Zhao, J.A. Paradiso, Energy efficient control of polychromatic solid state lighting using a sensor network, in: Society of Photo-Optical Instrumentation Engineers (SPIE) Conference Series, volume 7784 of Society of Photo-Optical Instrumentation Engineers (SPIE) Conference Series, 2010, pp. 778408–778408-15, August.
[5] V. Singhvi, A. Krause, C. Guestrin, J.H. Garrett Jr., H.S. Matthews, Intelligent light control using sensor networks, in: Proceedings of the 3rd International Conference on Embedded Networked Sensor Systems, SenSys'05, ACM, New York, NY, USA, 2005, pp. 218–229.
[6] V.H.C. Crisp, Preliminary study of automatic daylight control of artificial lighting, Lighting Research and Technology 9 (1) (1977) 31–41.
[7] D.R.G. Hunt, Simple expressions for predicting energy savings from photoelectric control of lighting, Lighting Research and Technology 9 (2) (1977) 93–102.
[8] C. Machado, J.A. Mendes, Automatic light control in domotics using artificial neural networks, World Academy of Science, Engineering and Technology 44 (2008) 813–818, August.
[9] J.D. Foley, A. van Dam, S.K. Feiner, J.F. Hughes, Computer Graphics: Principles and Practice in C, 2nd ed., Addison-Wesley Professional, Boston MA, USA, 1995.
[10] A. Pandharipande, D. Caicedo, Daylight integrated illumination control of {LED} systems based on enhanced presence sensing, Energy and Buildings 43 (4) (2011) 944–950.
[11] H. Park, J. Burke, M.B. Srivastava, Design and implementation of a wireless sensor network for intelligent light control, in: 6th International Symposium on Information Processing in Sensor Networks, 2007. IPSN 2007, 2007, pp. 370–379, April.
[12] A. Guillemin, N. Morel, An innovative lighting controller integrated in a self-adaptive building control system, Energy and Buildings 33 (5) (2001) 477–487.
[13] B. Lee, M. Aldrich, J.A. Paradiso, Methods for measuring work surface illuminance in adaptive solid state lighting networks, in: Eleventh International Conference on Solid State Lighting. SPIE, 2011, p. 81230V.
[14] S. Afshari, S. Mishra, A. Julius, F. Lizarralde, J.T. Wen, Modeling and feedback control of color-tunable led lighting systems, in: Proceedings of the 2012 American Control Conference (ACC), 2012, pp. 3663–3668.
[15] A. Zukauskas, R. Vaicekauskas, F. Ivanauskas, R. Gaska, M.S. Shur, Optimization of white polychromatic semiconductor lamps, Applied Physics Letters 80 (2) (2002) 234–236, January.
[16] K.J. Dowling, B. Kolsky, The design of a spectrally tunable light source, in: Ninth International Conference on Solid State Lighting, 2009, pp. 742206–742206-12.
[17] S.W. Brown, C. Santana, P. Eppeldauer, Development of a tunable led-based colorimetric source, Journal of Research of the National Institute of Standards and Technology 107 (4) (2002) 363–371.
[18] S. Muthu, F.J. Schuurmans, M.D. Pashley, Red, green, and blue led based white light generation: issues and control, in: Industry Applications Conference, 2002. Conference Record of the 37th IAS Annual Meeting, vol. 1, 2002, pp. 327–333.
[19] A. Zukauskas, R. Vaicekauskas, F. Ivanauskas, H. Vaitkevicius, P. Vitta, M.S. Shur, Statistical approach to color quality of solid-state lamps, IEEE Journal of Selected Topics in Quantum Electronics 15 (5) (2009) 1542, september/october.
[20] C. Starr, C.A. Evers, L. Starr, Biology: Concepts and Applications, 8th ed., Cengage Learning, KY, USA, 2010.
[21] H. Bai, M. Arcak, J.T. Wen, Cooperative Control Design: A Systematic, Passivity-Based Approach, Springer, New York, NY, 2011.
[22] P. Sen, S. Darabi, Compressive dual photography, Computer Graphics Forum 28 (2) (2009) 609–618.
[23] D.L. MacAdam, Visual sensitivities to color differences in daylight, Journal of the Optical Society of America (1917–1983) 32 (1942) 247, May.
[24] J. Schanda, Colorimetry, Understanding the CIE System, John Wiley & Sons, NJ, USA, 2007.
[25] P.R. Boyce, Human Factors in Lighting, 2nd ed, CRC Press, Abingdon, 2003.
[26] A.A. Kruithof, Aanslag van het waterstofmolecuulspectrum door electronen, Utrecht University, 1934, PhD thesis.
[27] R.C. Aster, B. Borchers, C.H. Thurber, Parameter Estimation and Inverse Problems, 2nd edition, Elsevier, 2013.
[28] S. Afshari, S. Mishra, J.T. Wen, R. Karlicek, Demo abstract: an adaptive smart lighting system, in: Proceedings of the 2012 Buildsys Conference, 2012, pp. 201–202.
[29] LED downlight, vivia round. http://www.gothamlighting.com/product/detail.aspx?id=119170
[30] Ocean optics, colorbug color measurement appliance. http://www.oceanoptics.com/products/colorbug.asp
[31] J. Wason, J.T. Wen, Robot raconteur: a communication architecture and library for robotic and automation systems, in: IEEE International Conference on Automation Science and Engineering, 2011, pp. 761–766, August.